

## Crustal Strains in the Eastern Mediterranean and Middle East as Derived from GPS Observations

Gamal S. EL-FIKY\*

National Research Institute of Astronomy and Geophysics, Helwan, Cairo, Egypt.

\* Present address: Earthquake Research Institute, The University of Tokyo

### Abstract

Velocity vectors estimated by GPS observations in the Eastern Mediterranean and Middle East region were used to investigate the crustal strain distribution in this region. Nine years of data from 1988 to 1997, estimated by McCLUSKY *et al.* (2000) were used to derive principal components of strains. We employed the Least-Squares Prediction (LSP) technique to segregate signals and noise in the data. Estimated signals were used to reconstruct the strains; dilations, maximum shear strains, and principal axes of strains. Results of crustal strains clearly portray active tectonic strains in the study region.

There are large convergent strain rates in the Mediterranean Sea, along the Hellenic Arc and south of it, which are directly related to the subduction of the African plate along this arc. Large extension strain rates with orientations varying between NNE-SSW and N-S are found in northern Aegean Sea and northwestern Anatolia. The southern Aegean Sea is characterized by relatively small strain rates.

Convergent strain rate is dominant in the northeastern Africa, but occurs at a relatively low rate. Patterns of strain rates located north and south of the Bitlis suture are quite similar, suggesting that most of the motion of Arabia is being transferred directly to Anatolia. East of the Karliova triple junction (KTJ), the compressional axes of strains show a tendency of being more easterly toward the NNE, resulting in shortening normal to the Caucasus thrust front. There is no indication of active deformation (almost strain-free) along the Cyprean Arc, south of Turkey, and near the Gulf of Iskenderum. Strain rates and level of earthquake occurrence are low in the central part of Anatolia, indicating that internal deformation in this region is very small. The principal axes of GPS strain rates show remarkable agreement with seismic data and fault plane solutions. In general, distinct seismic clusters accompany the areas of high geodetic strain rates, whereas the strain-free regions are nearly aseismic.

**Key words:** GPS data, Crustal strain, Eastern Mediterranean, Least-Squares Prediction, Plate motion

### 1. Introduction

The Eastern Mediterranean and Middle East region has been the focus of intense geological and geophysical investigations since the advent of modern Earth sciences (e.g., McKENZIE, 1970; Mueller and KAHLE, 1993). It is one of the most tectonically active areas on the Earth's surface (e.g., McKENZIE 1970, 1972, ARMIJO *et al.*, 1999). The tectonic framework of the Eastern Mediterranean and Middle East region is shown in

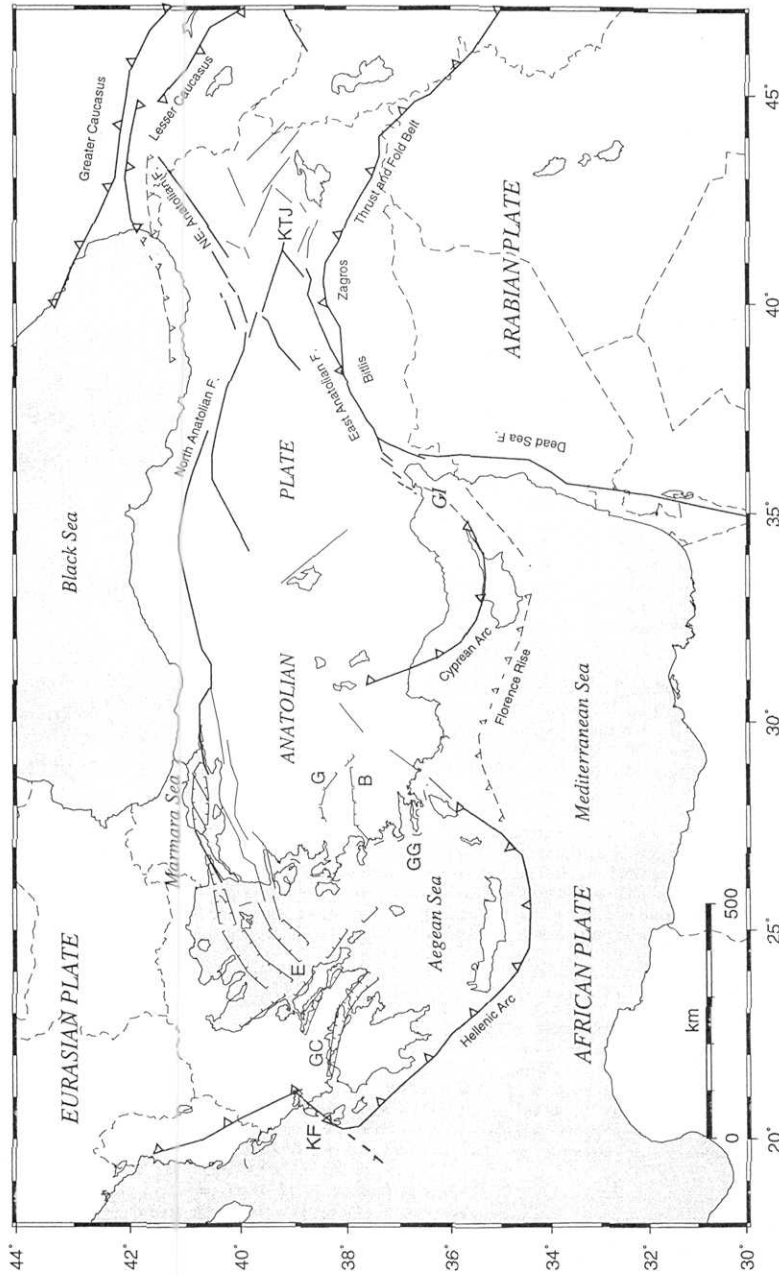


Fig. 1. Simplified tectonic map of the Eastern Mediterranean and the Middle East region. Solid lines are strike-slip faults, ticked lines are normal faults with ticks on the downthrown block, and lines with triangles are thrust faults on the overriding block. Dashed lines show international boundaries. Abbreviations are G, Gediz graben; B, Buyuk Menderes graben; E, Evia island; GC, Gulf of Corinth; GG, Gulf of Gokova; GI, Gulf of Iskenderum; KF, Kephallonia fault; and KTJ, Karlova triple Junction (modified from REILINGER *et al.*, 1997 a).

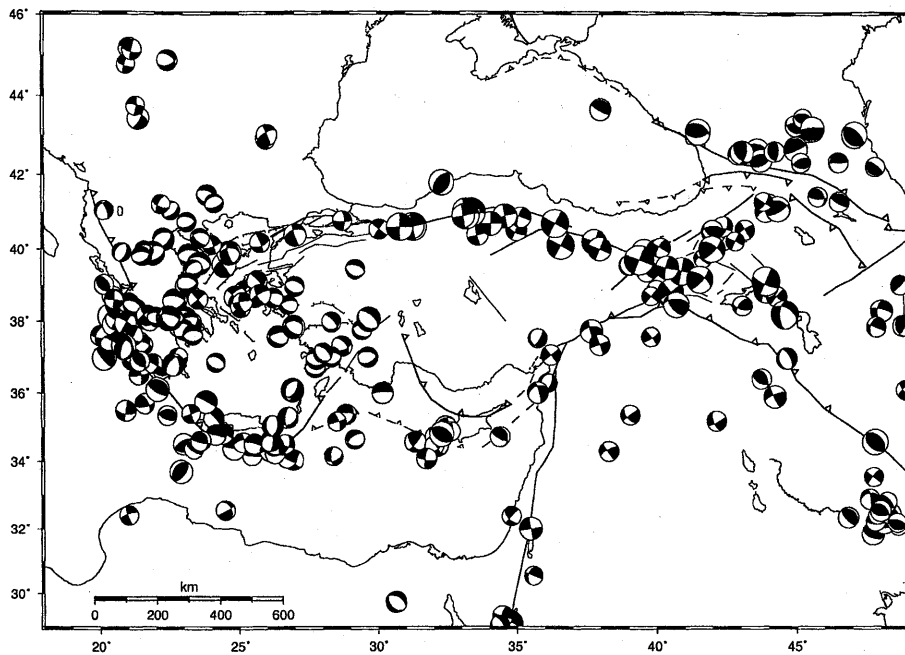


Fig. 2. Focal mechanisms (lower hemisphere projection) for shallow (depth of  $<100$  km), major earthquakes ( $M > 5.0$ ) (DZIEWONSKI *et al.*, 1981; JACKSON and MCKENZIE, 1988) in the Eastern Mediterranean region.

Fig. 1. This region has a wide variety of tectonic processes including various stages of continental collision (Zagros/Caucasus/Black Sea), subduction of oceanic lithosphere and associated back arc spreading (Cyprus/Hellenic/Calabrian arcs, Aegean and Tyrrhenian Seas), continental strike-slip faults (North and East Anatolian and Dead Sea faults), continental extension (western Turkey/Marmara Sea/Gulf of Corinth), major continental strike-slip faults (North and East Anatolian and Dead Sea faults), and a variety of smaller-scale processes associated with African-Arabian-Eurasian plate interactions. All of the above processes are contained within an area of approximately  $1000 \times 2000$  km<sup>2</sup>. Moreover, the Eastern Mediterranean region has a remarkably long historic record of major earthquakes (Fig. 2) (e.g., AMBRASEYS, 1975; AMBRASEYS and JACKSON, 1998).

The present-day geodynamic deformation in the Eastern Mediterranean results from the relative motion among three continental plates, namely: Eurasia, Africa, and Arabia (e.g., MCKENZIE, 1970). Plate motion models (DEMETS *et al.*, 1990; DEMETS *et al.*, 1994; JESTIN *et al.*, 1994) based on an analysis of earthquake slip vectors, seafloor spreading, and fault systems indicate that the Arabian plate is moving in a NNW direction relative to the Eurasian plate at a rate of about 20–25 mm/yr. These models also indicate that the African plate is moving in a northward direction relative to the Eurasian plate at a rate of about 10 mm/yr. Differential motion between Africa and Arabia ( $\sim 10$ –15 mm/yr) is thought to be taken up predominantly by left-lateral

motion along the Dead Sea transform fault (McCLUSKY *et al.*, 2000). The northward motion of the Arabian plate results in continental collision along the Bitlis-Zagros fold and thrust belt, earthquake activity (Fig. 2) and high topography in eastern Turkey and Caucasus mountains (Fig. 1), and westward extrusion of the Anatolian plate (McKENZIE, 1970; JACKSON, 1992; REILINGER *et al.*, 1997 a; ARMIJO *et al.*, 1999). The leading edge of the African plate is subducting along the Hellenic arc at a rate of  $\sim 40$  mm/yr, which is greater than the relative northward motion of the African plate itself (REILINGER *et al.*, 1997 a), requiring a southward movement of the Hellenic arc relative to the Eurasian plate (e.g., SONDER and ENGLAND, 1989; ROYDEN, 1993). On the other hand, the African plate is also thought to be subducting along the Cyprean arc and/or the Florence rise south of Turkey, although it is less well defined in these regions than along the Hellenic arc (e.g., JACKSON and McKENZIE, 1988).

Recently, there has been a significant improvement to the plate motion model for the Eastern Mediterranean region resulting from an analysis of seismic information, field studies of surface faulting, and air/satellite images. Using such data, JACKSON and McKENZIE (1988) and JACKSON (1992) have suggested that the Aegean Sea and Turkey consist of separate microplates with Turkey moving towards the west, relative to the Eurasian plate, at an average velocity of  $\sim 37$  mm/yr accommodated by an additional N-S deformation of  $\sim 11$  mm/yr in the Aegean, resulting in a total SW motion of  $\sim 41$  mm/yr. A large part of this deformation is seismic, as the Aegean shows a total seismic extension of the order of 20 mm/yr (PAPAZACHOS and KIRATZI, 1996). The recent space geodetic data analysis (e.g., ORAL *et al.*, 1992; LE PICHON *et al.*, 1995) has confirmed the westerly motion of the Anatolia plate.

Crustal deformation in the Middle East and Eastern Mediterranean is mainly occurring at the boundaries of three major plates, Eurasia, Africa, and Arabia, and the boundaries of microplates including Anatolian and Aegean. Attempts to quantify broad-scale plate motions and the detailed deformations associated with plate interactions in this region have used space geodetic observations, which were initiated in the region in the early 1980s (e.g., SMITH *et al.*, 1994; STRAUB and KAHLE, 1994, 1995; KAHLE *et al.*, 1995; LE PICHON *et al.*, 1995; NOOMEN *et al.*, 1996; REILINGER *et al.*, 1997 a, b; DAVIES *et al.*, 1997; PLAG *et al.*, 1998). In this study we use GPS velocity field compiled by McCLUSKY *et al.* (2000) for the period from 1988 to 1997, and applied the Least-Squares Prediction (LSP) technique for strain fields analysis developed by MORITZ (1962) for gravity data reduction and introduced for horizontal crustal strains by EL-FIKY (1998) and EL-FIKY and KATO (1999). We add a discussion on the results of strain fields in this tectonically active region, as well as along the boundaries of the above main and micro-plates, comparing them to the seismicity data and fault plane solutions.

## 2. GPS Velocity Field

GPS techniques have been rapidly developed and used for crustal deformation researches since around 1980 in various regions of the Earth. In the Eastern Mediterranean region, the GPS measurements were also initiated in 1988. The

campaign observations have been expanded and repeated in selected parts of the area each year between 1989 and 1997, except for 1995 (REILINGER *et al.*, 1997 a). There is a series of published papers concerning displacement field of the Eastern Mediterranean and Middle East based on GPS observations (e.g., KAHLE *et al.*, 1996; PETER *et al.*, 1998; REILINGER *et al.*, 1997 a; b; STRAUB *et al.*, 1997; and MCCLUSKY *et al.*, 2000). Among the several publications above, we employed MCCLUSKY *et al.* (2000), because it integrates all the GPS measurements in the region and gives the data set as a table. The data length spans over nine years, which is long enough to obtain reliable velocities at sites. According to MCCLUSKY *et al.* (2000), the Aegean region of Greece was observed in 1988/1989, 1992, and 1996 (for details also see KAHLE *et al.* 1996); in the West Hellenic Arc region of Greece, observations were made in 1989, 1990, 1991, 1992, 1993, 1994, and 1996; the 1996 West Hellenic Arc survey mainly included observations from stations from the new Continuous Ionian Network (CION) (PETER *et al.*, 1998); between 1988 and 1992, measurements were concentrated during alternate years in western and eastern Turkey, with a sufficient overlap to allow integration of the networks, but since the 1994 survey, almost all of the stations have been reoccupied during each survey (REILINGER *et al.*, 1997 a); in addition to these broad-scale surveys in Turkey a small and relatively dense network of stations spanning the various strands of the North Anatolian Fault (NAF) in the Marmara region was observed in 1990, 1992, 1994, and 1996 (STRAUB *et al.*, 1997); the Caucasus network was observed in 1991, 1994, and 1996 (REILINGER *et al.*, 1997 b). Regarding the northeastern edge of the African plate, three stations located on Egypt were observed over a three-year period (1994–1997). Altogether, 189 stations in total were observed in the Eastern Mediterranean-Middle East region during the period 1988–1997. Fig. 3 reproduces velocity field derived from GPS observation by MCCLUSKY *et al.* (2000). The velocity field in this figure is relative to the Eurasian plate, which is defined by minimizing the horizontal velocities of 16 stations in Western Europe and central Asia. As is readily seen in this figure, there is a counterclockwise rotation of central/western Turkey and the southern Aegean/ Peloponnisos. Northward motions of northeastern Africa as well as the northern part of the Arabian plate are also clearly seen in the figure.

Monitoring the crustal strain perturbations in space and time is a key to understanding the physical process in the crust, as well as forecasting crustal activity. Dense GPS measurements with long time spans provide us with one of the ideal tools to realize this. In the present study, we try to delineate the crustal strain of the Eastern Mediterranean using above dense GPS measurements in the data period and discuss its tectonic implications.

### 3. Strains Analysis

To delineate crustal strains in the Eastern Mediterranean and Middle East region, we applied the Least-Squares Prediction (LSP) method used by EL-FIKY and KATO (1999). The method is a corollary of the least-squares collocation method developed by MORITZ (1962) for the reduction of gravity data. In this method EL-FIKY and KATO (1999) assumed that the spatially distribution of geodetic data  $l$  is given by

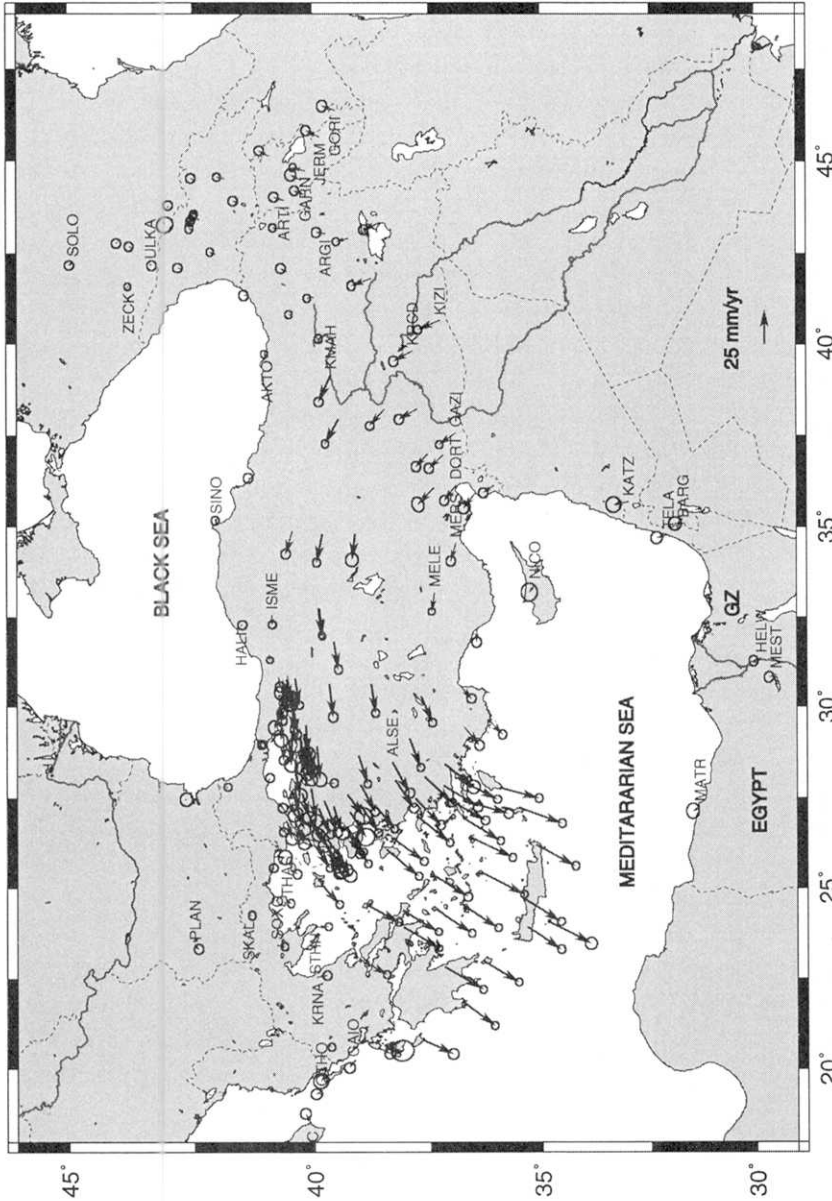


Fig. 3. Velocity field estimated from repeated GPS observations and its 95% confidence ellipses in Eurasia-fixed reference frame for the period from 1988 to 1997 (McClusky *et al.*, 2000). GZ is stand for Gulf of Suze.

the summation of tectonic signal  $t$  and noise  $n$  so that it is expressed by the following observation equation;

$$l = t + n.$$

Where  $t$  is the tectonic signal vector at the observation points and  $n$  is the noise vector, which represents the measuring error. Here, the signal is the tectonic deformation that arises from inside and outside the region. Noise is generated from erroneous fluctuations that are inherent in each of the GPS sites. Such noise stems from known or unknown sources such as monument instability, underground water flow, or other artificial causes. This noise may have to be removed to obtain the crustal deformation of the tectonic origin. Thus, the problem is to extract the signal  $S$  at any arbitrary location from  $l$  using a filtering technique, considering that noise  $n$  is limited only to the site or adjacent local regions and tectonic signal  $t$  may have rather wider correlations in nature (EL-FIKY and KATO, 1999). Thus, the hypothesis in which the signal has a spatial correlation whereas the noise does not is made use to separate them components. Variance-covariance analysis of data is a good measure to find such spatial correlation. If we assume that the velocity field is isotropic and homogeneous, the covariance of data is only a function of site distance (e.g., EL-FIKY *et al.*, 1997). We then demean the EW and NS velocity components and calculate the variance  $C_l(0) = (\sum l_i l_i) / N$  and covariance  $C_l(d_q) = (\sum l_i l_j) / N_q$  of the data for each component. Here,  $N$  is the total number of data sites and  $N_q$  is the number of data points within a specific discrete distance interval, from which  $d_q$  is taken as the median of this assumed interval. Variances are estimated at each observational site, whereas covariances are estimated for all site pairs within the assigned distance interval. Thus obtained variances  $C_l(0)$  may include signal and noise, but the covariances  $C_l(d_q)$  include only signals according to the above hypothesis.

The plot of the covariances with respect to distance would be a curve that naturally diminishes with distance. One simple mathematical function to express such plots would be a Gaussian function in the following form,  $C_l(d_i) = C_l(0) \exp(-k^2 d_i^2)$ , which we choose here as the empirical covariance function (ECF). Two parameters  $C_l(0)$  and  $k$  are fitted from a covariance plot of the data.  $C_l(0)$  is the expected variance at the sites and  $C_r(0) = C_l(0) - C_t(0)$  is considered the noise component at the site.  $k$  is an indication of how far the correlation reaches, which has the dimension of inverse distance.

The obtained variance-covariance plot and fitted ECF are shown in Fig. 4. The east-west component where  $C_{lu}$  is the variance-covariance of velocity vectors and the north-south component where  $C_{lv}$  is the variance-covariance for this component are shown in Fig. 4 (a) and Fig. 4 (b), respectively.

Once such ECF is obtained, we can estimate signal  $S$  at any arbitrary point from the following formula (e.g., EL-FIKY and KATO, 1999);

$$S = C_{st} C_L^{-1} l.$$

Where the matrix  $C_{st}$  is composed of elements  $c_{st}$  ( $1 \leq t \leq N$ ,  $1 \leq s \leq P$ , where  $P$  is the number of grid points whose signals are to be estimated);  $c_{st}$  is given by  $c_{st} = C_{ut}(0) \exp(-k_u^2 d_{st}^2)$  for EW component and  $c_{st} = C_{vt}(0) \exp(-k_v^2 d_{st}^2)$  for NS component, respectively,

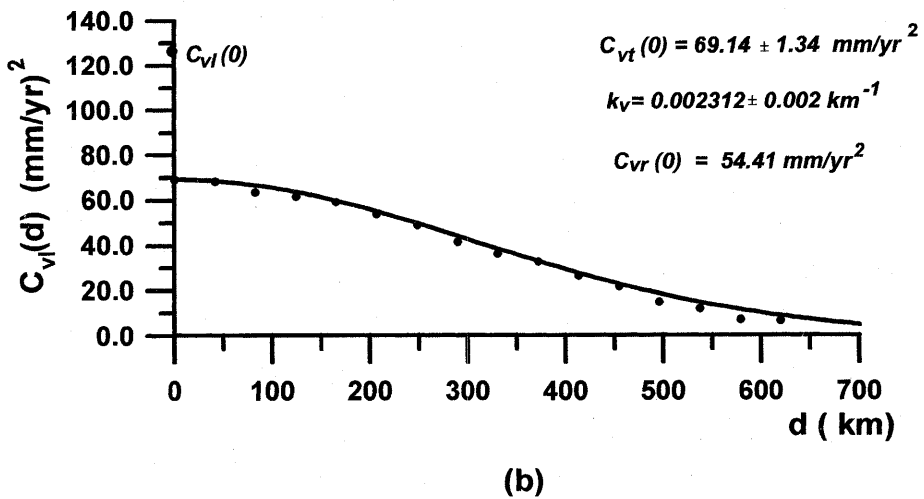
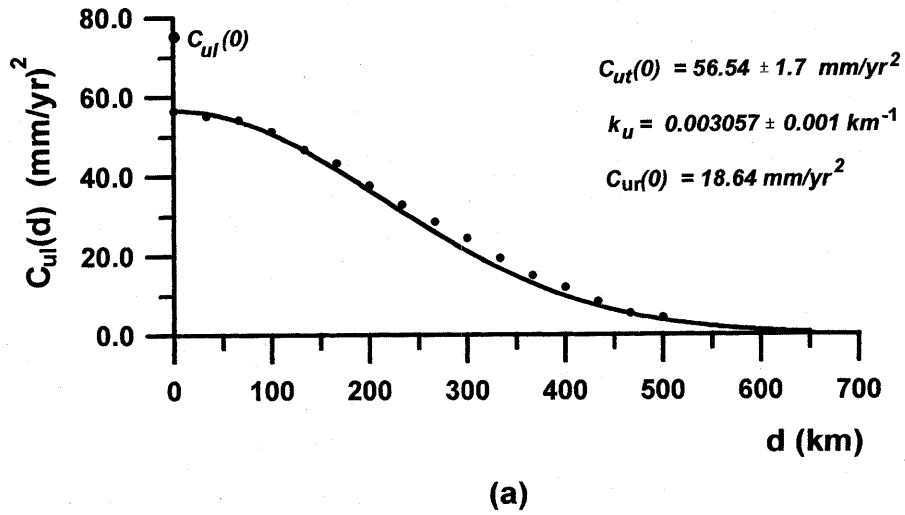


Fig. 4. Variance- covariance of displacement vectors for discrete baseline distances and fitted empirical covariance functions; (a) EW component, and (b) NS component, respectively. Estimated parameters ( $C_{uf}(0)$ ,  $C_{un}(0)$  and  $k_u$ ) for EW component and ( $C_{vf}(0)$ ,  $C_{vn}(0)$  and  $k_v$ ) for NS component are shown in the figure.

where  $d_{st}$  is distance between the data site and the predicted site. The above formula was used to reconstruct velocity vectors (signal) at grid points of  $10 \text{ km} \times 10 \text{ km}$  mesh covering the study region.

#### 4. Results and discussion

Before applying LSP, systematic bias is removed from all site velocities by



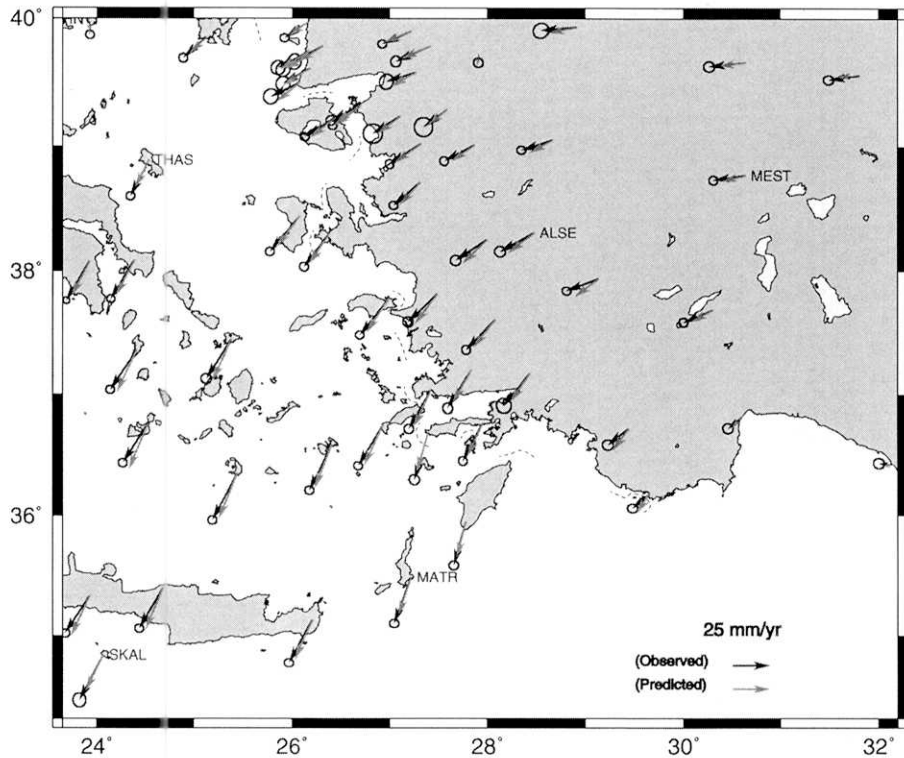


Fig. 5. Observed GPS horizontal displacement vectors and its 95% confidence ellipses at some sites (black arrows) and predicted one by LSP (grey arrows) for the period from 1988 to 1997.

subtracting the average of velocities. Then, we applied the LSP as described above to each of the vector components (East-West and North-South) independently. Thus the obtained variance-covariance plot and fitted ECF are shown in Fig. 4. ECF for each of the components are fitted to the data. Estimated parameters (EW:  $k_u$ ,  $C_{ub}$ , NS:  $k_v$  and  $C_{vt}$ ) are used to compose the covariances matrices, which can be further used to reconstruct displacement vectors (signal) at grid points in the Eastern Mediterranean region (Fig. 4). Then estimated velocities at these grid points are differentiated in space to obtain crustal strains in this data period.

The obtained covariance functions (Figs. 4a and 4b) approach zero at distances of 500 km and 620 km for EW component and for NS component, respectively. These correlation distances are about three times greater than one of East Asia (Japanese islands) (KATO *et al.*, 1998). This might indicate that the characteristic wave-length of crustal deformations or crustal blocks are a little less fragmented in the Eastern Mediterranean region compared with to Japanese islands.

In Fig. 5, we compare the smoothed displacement vectors obtained at some data points estimated by LSP with the observed one. As is readily seen in Fig. 5, the observed horizontal displacements and those estimated by LSP are approximately

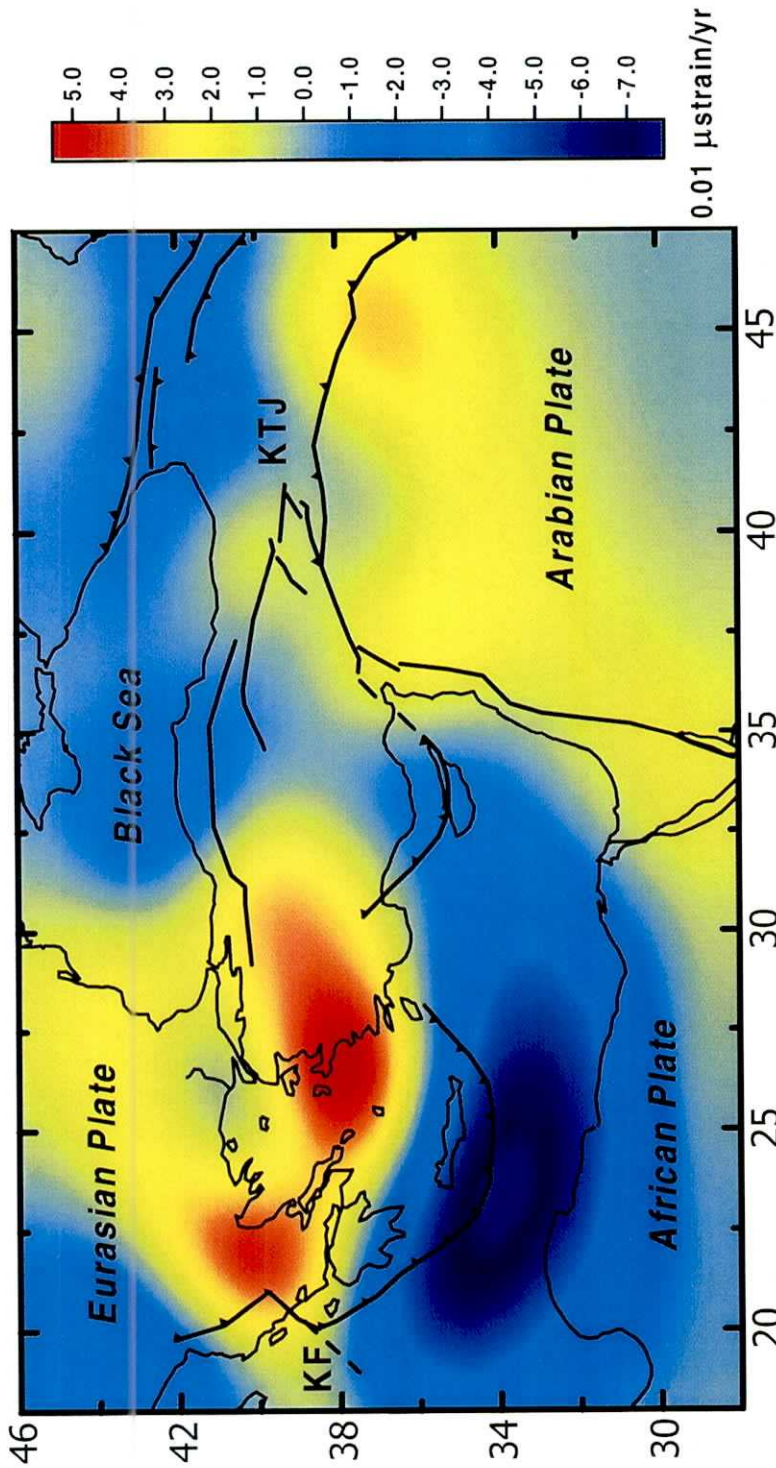


Fig. 6. The areal dilatation of the Eastern Mediterranean and Middle east region estimated by the LSP technique for the period from 1988 to 1997. Unit is  $0.01 \times \text{strain/yr}$ .

the same over the area, but some differences exist.

Figs. 6, 7, and 8 are estimated areal dilatational strains, maximum shear strains, and principal axes of strains, respectively. These figures, though estimated from only nine years of data, may well portray the characteristics of the tectonic strains in the Eastern Mediterranean region.

In northeastern Africa, convergent strain rate is dominant (Figs. 6 and 8), but it occurs at a relatively low rate. This might be due to the subduction of the African plate along the Hellenic arc and/or Cyprean arc. Maximum shear strain in the western part of this region reaches  $0.04\mu\text{strain/yr}$  and compressional axes oriented in N-S. The three stations located on the northeastern edge of the African plate (HELW, MEST, and MATR) used in this study were observed over only a three-year period (1994-1997). On the other hand, the displacement vectors of these stations have high uncertainties. Therefore, the reported motions (Fig. 3) are not so reliable for providing a useful constraint on the Africa plate motion. These stations show a northward motion relative to the Eurasian plate at rates of  $6\pm 2$ ,  $5\pm 2$ , and  $6\pm 4$  mm/yr, respectively. This is about half of the rate determined by NUVEL-1A ( $10\pm 1$  mm/yr at  $N2^\circ \pm 2^\circ E$ ).

The strain rates along the Dead Sea fault around station BARG in Fig. 3, are very low or almost strain-free. The displacement rate of this station, 7 mm/yr, is also slower than the rate estimated for African plate by NUVEL-1A ( $11\pm 1$  mm/yr in  $N2^\circ \pm 3^\circ E$  direction). The satellite laser ranging (SLR) observations near HELW and BARG supported those low GPS rates for northeastern Africa (ROBBINS *et al.*, 1995). The problem with SLR observations is that the results have high uncertainties at these locations (Helwan,  $6\pm 9$  mm/yr at  $213^\circ \pm 62^\circ$ ; Bar Giyyora,  $9\pm 3$  mm/yr at  $12^\circ \pm 53^\circ$ ). Thus, the significance of these observations for overall African plate motion is difficult to determine, because of the possible effects of the Dead Sea fault and/or the Sinai microplate (e.g., COURTILLOT *et al.*, 1987). On the other hand, the GPS velocity field (Fig. 3) suggests possible motion across the Gulf of Suze (GZ in Fig. 3) (e.g., JOFFE and GARFUNKEL, 1987) and the Sinai block (i.e., HELW/MEST and BARG/TELA). In fact, long span and denser GPS observations are needed to clarify both the low strain rate and slow rate for northeastern Africa as well as possible motion of the Sinai block relative to Africa.

Along the Bitlis suture, the collision zone between the Arabian and Anatolian plates, the strain rates are very low. The velocity field of three sites (KIZI, KRCD, GAZI), located south of the Bitlis suture on the northern edge of the Arabian plate shows a NW motion relative to Eurasia ( $18\pm 2$  mm/yr in  $N24^\circ \pm 5^\circ W$  direction;  $16\pm 2$  mm/yr in  $N32^\circ \pm 5^\circ W$  direction; and  $15\pm 2$  mm/yr in  $N40^\circ \pm 5^\circ W$  direction, respectively) slightly slower and more westward than NUVEL-1A estimates ( $25\pm 1$  mm/yr in  $N21\pm 5^\circ W$  direction at KIZI). The slower GPS rates may indicate that stations along the northern edge of Arabia are involved in the Arabia-Anatolia deformation and/or that crustal shortening occurs within the Arabian plate to the south, possibly in the Palmyrides (e.g., CHAIMOV *et al.*, 1990). On the other hand, the patterns of strain rates (Figs. 6~8) located north and south of the Bitlis suture are quite similar,

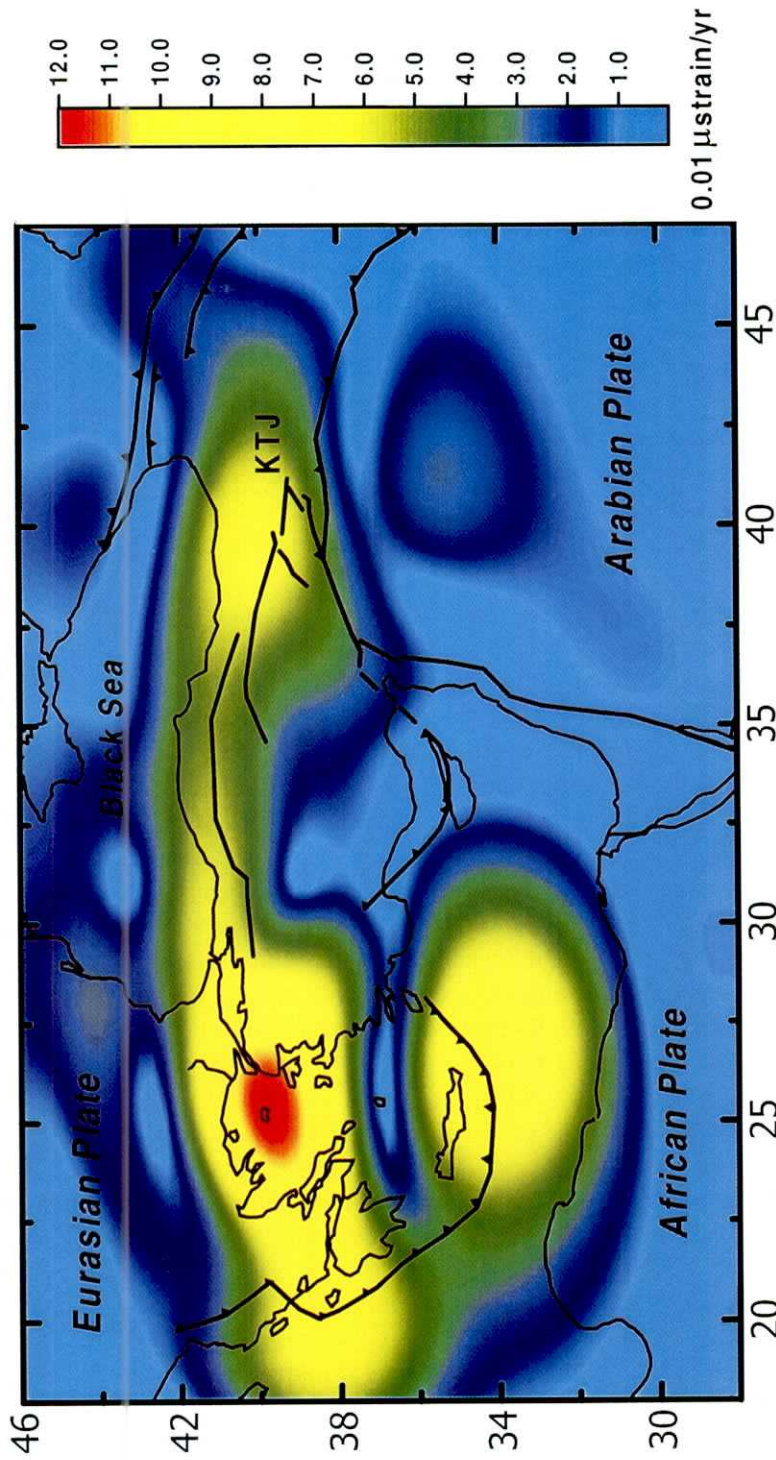


Fig. 7. Distribution of the maximum shear strain in the Eastern Mediterranean and Middle east region estimated by the LSP technique for the period from 1988 to 1997. Unit is  $0.01 \times \text{strain/yr}$ .



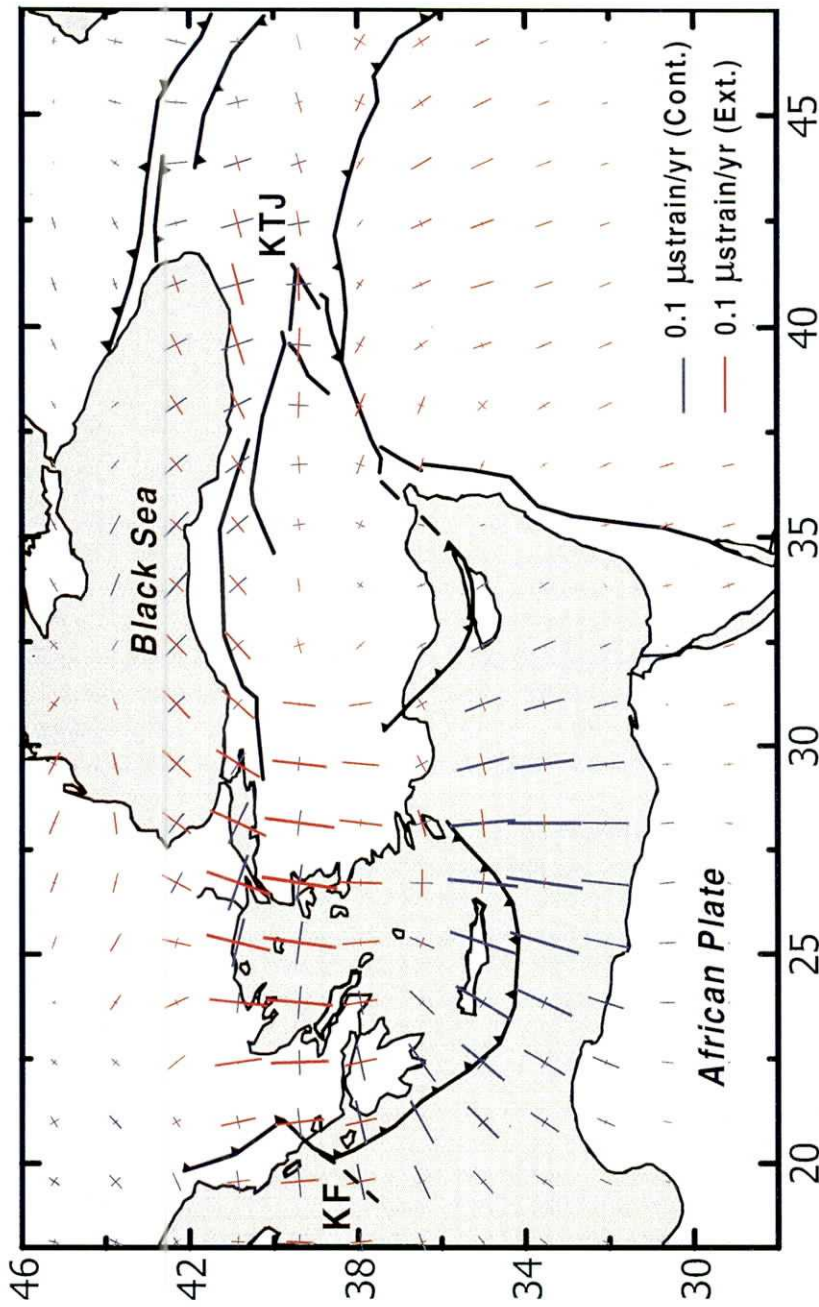


Fig. 8. Magnitude and orientation of principal axes of strains in the Eastern Mediterranean and Middle East region estimated by the LSP technique for the period from 1988 to 1997. Blue bars are compressional and red bars are extensional strains, respectively. Unit is  $0.01 \times$  strain/yr.

suggesting that most of the motion of Arabia is being transferred directly to Anatolia.

The present study shows that there is no indication of active deformation or there is almost a strain-free condition (Figs. 6~8), along the Cyprean Arc, south of Turkey, and near the Gulf of Iskenderum (Fig. 1). The absence of active deformation in this region has already been noted by McCLUSKY *et al.* (2000) from the GPS velocity field.

The Dead Sea fault, the East Anatolian Fault, and the Cyprus arc are three zones that accommodate deformation between Africa and Arabia, Turkey and Arabia, and Turkey and Africa, respectively. The level of seismicity was too low in the last century to draw any firm conclusions in the above three zones (JACKSON and McKENZIE, 1988). Historical seismicity is known from all three zones, with occasional large ( $M > 7.3$ ) earthquakes on the East Anatolian and Dead Sea faults (AMBRASEYS, 1975). On these large strike-slip faults a substantial part of the deformation may occur through large, relatively infrequent earthquakes every few hundred years, as seen with similar faults elsewhere, rather than through the more frequent  $M = 6.0 - 7.0$  earthquakes that characterize the rest of the Mediterranean-Middle East region. The present GPS data analysis shows that the strain rates are low on the East Anatolian Fault and almost strain-free along the Dead Sea fault and the Cyprus arc.

In eastern Turkey, east of the Karliova triple junction (KTJ) to north ( $\sim 41^\circ$  E longitude), the compressional axes of strains (Fig. 8) tend to rotate gradually from NNW to more easterly directions toward the NNE, resulting in shortening more or less normal to the Caucasus thrust front in Armenia and Georgia. In contrast, the compressional axes west of the KTJ show a tendency to align in a more westward direction.

East Turkey and the Caucasus is a zone of widespread deformation separating Arabia and Eurasia. A study of historical and instrumental seismicity made by GORSHKOV (1984), in which magnitudes are estimated for all earthquakes with  $M > 5.0$ , shows that no earthquake of a magnitude larger than 7.0 has occurred since 1800 in this region. The determination of the maximum possible earthquake made by RIZNICHENKO and DZHIBLADZE (1974) also gives the same results. On the basis of the GORSHKOV catalogue, PHILIP *et al.* (1989) obtained a Gutenberg-Richter law of the form:  $\log N = 6.07 - 0.79 M$  ( $5 < M < 7$ ) for the region including Great and Lesser Caucasus and for the period 1900-1980, in which data may be considered to be more or less homogeneous. On the other hand, the velocity of shortening and the rate of strain from the accumulated sum of seismic moments of earthquakes in this region are estimated to be 1.3 mm/yr and about  $0.005 - 0.007 \mu\text{strain/yr}$ , respectively (JACKSON and McKENZIE, 1988; PHILIP *et al.*, 1989). The present analysis shows that the compressional strain reached  $0.06 \mu\text{strain/yr}$  in this region. This is about one order of magnitude higher than that attributed to earthquakes. The difference could be due to aseismic deformation.

There are large, convergent strain rates in the Mediterranean Sea, along the Hellenic Arc and south of it (Figs. 6 and 8), which is directly related to the accommo-

dation of  $\sim 40$  mm/yr of shortening between the Island of Crete and the northern Africa as inferred from the GPS velocity field (Fig. 3). Maximum shear strain rates in this region reach  $0.11 \mu\text{strain/yr}$  and compressional axes oriented in SW-NE. Large principal values of strain rates are found in northern Aegean Sea and northwestern Anatolia passing the northern part of the Marmara Sea, reaching principal rates of extension of  $0.12 \mu\text{strain/yr}$  at the western end of NAF zone, and  $0.13 \mu\text{strain/yr}$  at the North Aegean Trough (NAT). On the other hand, the GPS strain field along the NAF is clearly visible (Figs. 7 and 8). The southern Aegean Sea and central Anatolia have low strain rates or are almost strain-free. The low strain rates and low level of earthquake occurrence (Fig. 2) in central of Anatolia indicate that internal deformation in this region is very small. The principal axes of GPS strain rates in the northern Aegean Sea are consistent with those estimated by JACKSON *et al.* (1992) from seismic data.

In western Anatolia, N-S oriented principal values of extension on the order of 0.1 to  $0.12 \mu\text{strain/yr}$  dominate, with orientation varying between NNE-SSW and N-S. They are accompanied by normal faulting earthquake mechanisms (Fig. 2) with the  $\sigma_3$  axes oriented mostly in the same direction as the GPS derived principal axes of extension. In southwest Anatolia, segments of the seismic activity associated with the west Anatolian graben system can be identified. This zone comprises the Gediz, Medderes, and Gokova grabens, as well as the Fethiye-Burdur zone, which shows NW-SE oriented rifting with a rate of  $0.09 \mu\text{strain/yr}$ . In the southeast Aegean Sea a distinct seismic cluster is visible. This area of extension is seen from the GPS results with a rate of  $0.09 \mu\text{strain/yr}$ . The focal mechanisms in the southern Aegean are characterized by thrust faulting with a significant strike-slip component (TAYMAZ *et al.*, 1991). The trend of the compressional axes derived from GPS is perpendicular to the arc.

Mainly from geological data and earthquake focal mechanisms, MULLER *et al.* (1992) and ZOBACK (1992) compiled stress data for the Aegean Sea and western Anatolia. These studies show dominant N-S extension in western Anatolia and in the Aegean. Even though data east of  $30^\circ\text{E}$  show more scatter for compressive horizontal stress ( $S_{H\text{max}}$ ) orientations, they clearly show a change of deformation style to a more strike-slip type (MULLER *et al.*, 1992). The Hellenic arc is associated with  $S_{H\text{max}}$  orientation consistent with SSW convergence direction between the Aegean Sea region and Africa. In spite of the scattering of data and the uneven distribution of sampling sites, the overall pattern is in general agreement with the strain rate field derived from GPS (Fig. 8), showing strong compression perpendicular to Hellenic arc. In addition, the present study indicates a relatively strain-free region in the central southern Aegean (Figs. 6~8), between the volcanic ( $37^\circ$  to  $38^\circ\text{N}$ ) and the non-volcanic Hellenic arc ( $35^\circ$  to  $36^\circ\text{N}$ ). On the other hand, the high extensional strain rates in the northern Aegean Sea and in the western Anatolia are consistent with the stress map of MULLER *et al.* (1992).

Based on fault plane solutions, TAYMAZ *et al.* (1991) showed that the northern and central Aegean area is governed by distributed right lateral strike-slip faulting

trending NE to ENE. Normal faulting created several prominent basins at the eastern end of the North Aegean Trough. The GPS strain rate analysis reveals that extensional strains with orientation varying between NNE-SSW to N-S dominate this region (Fig. 8).

Components of strain rate tensors based on seismic moment tensor summation have been recently re-estimated by PAPAACHOS and KIRATZI (1996) and converted into velocities using 63 seismogenic sources in the Aegean and surrounding area. The deformation along the coast regions of Albania and northwestern Greece down to the Kephallonia Fault (KF) (Fig. 1) is taken up by compression in a direction perpendicular to the coast line, at a rate of 4 mm/yr in a direction N49°E. The right-lateral strike-slip Kephallonia Fault demarcates the beginning of the Hellenic subduction zone. Nearly all seismic events that have occurred south of it, along the Hellenic arc, have dominant dip-slip thrust mechanisms (Fig. 2). The compressional strain accumulation along the Hellenic arc is also seen in the GPS results (Fig. 8).

Extensional strains in the Aegean Sea and surrounding area have been confirmed by the new inversion of seismic events of PAPAACHOS and KIRATZI (1996). Their results show extension deformation in this region. Its direction shows an anticlockwise rotation in the northern part of this area from east to west. This extension has a NNE direction in northwestern Anatolia, a NNW direction in the central and northern Greece, as well as along the southern volcanic arc, and a WNW direction in the westernmost part of the Anatolia. On the other hand, JACKSON *et al.* (1992, 1994) determined the horizontal velocity field from the spatial distribution of seismic moment tensor of earthquakes in the Aegean region. They found E-W right-lateral shear in northwestern Anatolia related to motion on the NAF, becoming distributed as it enters the northern Aegean Sea. Further south, toward the volcanic chain, they identified N-S extension. In the eastern Aegean seismicity does not account for the geodetic strain rates observed. JACKSON *et al.* (1994) postulated that a seismic strain deficit or aseismic slip may exist in the eastern Aegean, as well as in central Greece. Our strain analysis confirms this observation for central and northern Greece in particular. In a seismic hazard assessment it is important to evaluate which of the two reasons, strain deficit or aseismic slip, is responsible for this discrepancy.

Strain rates throughout northern Greece are relatively high (Figs. 6~8), and show a generally north-south extension (typically around  $0.11 \mu\text{strain/yr}$ ); extensional strain rates within southern Greece (Peloponnesos) are relatively low. Based on seismicity data and fault-plane solutions for southern Italy, ANDERSON and JACKSON (1987) showed that active deformation varies between N-S shortening and NE-SW extension on normal faults along the Apennine Chain. The Dinaric coast region, north Greece, is deforming along strike-slip and thrust faults. A belt of NE-SW-shortening continues into northwestern Greece with numerous transcurrent fault systems. E-W-oriented compressional axes of strains are seen in this region in the present GPS analysis. Maps of in-situ stress measurements compiled by REBAI *et al.* (1992) mainly show N-S extensional stress ( $S_{Hmax}$ ) in central Greece, which is also seen in the GPS results (Figs. 6~8).



The southwestern margin of Greece is dominated mainly by the subduction of the African plate along the Hellenic trench. The most important fault zone taking up this motion is the right-lateral Kephallonia Fault (KF) (Fig. 1). It separates GPS sites to the north of it, which show a negligible velocity field relative to the Eurasian plate (Fig. 3), from sites south of it, which show rapid movement to SW. The variation in direction and magnitude of principal axes of strains around of the KF is clearly seen in Fig. 8.

AMBRASEYS and JACKSON (1990) have examined the seismicity of Greece for the period from 1890 to 1988. They concluded that the distribution of large earthquakes in the 100-year interval is comparable to the last 25-year interval. The most striking feature of the seismicity of the longer period is the intense activity in the Gulf of Corinth (GC in Fig. 1) and between the island of Evia (E in Fig. 1) and the Greek mainland. The present GPS results reveal that this region is characterized by a large extensional strain. Maximum extension occurs near the region of the graben-type plains in northern central Greece, which was the site of several strong normal faulting earthquakes in 1954 (PAPASTAMATIOU and MOUYARIS, 1986), in 1957, and in 1980 (PAPAZACHOS *et al.* 1992). Average rates based on seismic moment release for northern central Greece were estimated as 10 mm/yr in the N6°W direction (PAVLIDES *et al.*, 1995). This rate is considerably smaller than the one obtained from GPS data (KAHLE *et al.*, 1995). Maximum strain rate estimated by AMBRASEYS and JACKSON (1990) is 0.07  $\mu$ strain/yr, whereas it is about 0.11  $\mu$ strain/yr from the present GPS analysis. This discrepancy might be due to aseismic strain release or an apparent seismic strain deficit because of the short time interval considered for the moment summation.

The present analysis shows that northern Anatolia is dominated by both extensional and compressional strain rates (Fig. 8). This might be due to the restraining and releasing of stress along the NAF, which changes its strike on several well-defined fault segments (BARKA, 1992). BARKA and KADINSKY-CADE (1988) present detailed geological and seismological descriptions of NAF, including estimates of slip rates, age of the current fault configuration, and total fault offset. Briefly, NAF extends from KTJ in east to the Marmara Sea. Dextral slip associated with this 1200 km long fault appears to extend into the North Aegean Sea and possibly connects in some complex way with the right-lateral Ionian transform fault (Fig. 1) (KAHLE *et al.*, 1995). Rates of slip on NAF are estimated from geological data between 5 and 15 mm/yr (BARKA and KADINSKY-CADE, 1988) and from GPS data between 24 and 30 mm/yr (McCLUSKY *et al.*, 2000; REILINGER *et al.* 1997 a). The discrepancy between the GPS and geological slip rate estimates suggests that total fault offset might be substantially underestimated and/or that perhaps as much as half of the Anatolia-Eurasia relative motion is taken up by unidentified faults or by an elastic deformation of the adjacent plates. In the last 80 years most of NAF ruptured in a spectacular series of M=7–8 earthquake (e.g., AMBRASEYS, 1970). Focal mechanisms for these and other moderate to large earthquakes indicate predominantly pure right-lateral strike slip along the eastern and central segments of the fault transitioning into a combination of right-lateral and extensional mechanisms along the western segment in the region of the

Marmara Sea (Fig. 2).

## 7. Conclusions

The velocity vectors derived from GPS observations in the Mediterranean-Middle East region estimated by McCLUSKY *et al.* (2000) for GPS data during 1988 to 1997 were used to investigate crustal strains distribution in this tectonically active region. The Least-Squares Prediction technique was employed to segregate signal and noise in the observed displacements vectors. Estimated signals were used to reconstruct the strains; dilatations, maximum shear strains, and principal axes of strains. The crustal strains estimated from nine years of GPS data accurately portray the characteristics of the active tectonic strains in this region.

Large convergent strain rates are found along the Hellenic Arc, which might be related to the subduction of the African plate along this arc. Central Anatolia is strain-free, whereas northern Aegean Sea and northwestern Anatolia are mainly occupied by NNE-SSW and N-S oriented extension. The southern Aegean Sea is characterized by relatively small strain rates.

The internal deformation in the Anatolian plate is very small. Patterns of strain rates along Bitlis suture suggests that most of the motion of Arabia is transferred directly to Anatolia. Compressional axes of strains show a tendency of being more easterly toward the NNE east of the Karliova triple junction (KTJ), resulting in a shortening normal to the Caucasus thrust front. There is no indication of active deformation, or almost a strain-free condition, along the Cyprean Arc, south of Turkey, and near the Gulf of Iskenderum. The principal axes of GPS strain rates are in agreement with those of seismic data and fault plane solutions. Generally, distinct seismic clusters accompany the areas of high geodetic strain rates, whereas the low strain rates regions are nearly aseismic.

## Acknowledgments

Prof. Teruyuki KATO and Dr. Shinji TODA, both at the Earthquake Research Institute, the University of Tokyo, reviewed the manuscript and gave valuable comments to the author. A GMT software package was used to plot some figures. The author is grateful to the Japan Society for the promotion of science (JSPS) for supporting him during this study.

## References

- AMBRASEYS, N.N., 1975, Studies in historical seismicity and tectonic, In *Geodynamics today: A Review of the Earth's Dynamic Processes*, pp. 7-16, Royal Society, London.
- AMBRASEYS, N.N. and J.A. JACKSON, 1990, Seismicity and associated strain of central Greece between 1890 and 1988, *Geophys. J. Int.*, **101**, 663-708.
- AMBRASEYS, N.N. and J.A. JACKSON, 1998, Faulting associated with historical and recent earthquakes in the Eastern Mediterranean region, *Geophys. J. Int.*, **133**, 390-406.
- ANDERSON, H. and J. JACKSON, 1987, Active tectonics of the Adriatic region, *Geophys. J.R. Astron. Soc.*, **91**, 937-983.
- ARMLJO, R., B. MEYER, A. HUBERT and A. BARKA, 1999, Westward propagation of the North

# Crustal Strains in the Eastern Mediterranean and Middle East as Derived from GPS Observations

- Anatolian fault into the northern Aegean: Timing and kinematics, *Geology*, **27**, 267-270.
- BARKA, A., 1992, The North Anatolia fault zone, *Annales Tectonicae*, suppl. **6**, 164-195.
- BARKA, A. and K. KADINSKY-CADE, 1988, Strike-slip fault geometry in Turkey and its influence on earthquake activity, *Tectonics*, **7**, 663-684.
- BARKA, A. and R. REILINGER, 1997, Active tectonics of the Eastern Mediterranean region: Deduced from GPS, new tectonic, and seismicity data, *Ann. Geofis.*, **40**, 587-610.
- CHAIMOV, T.A., M. BARAZANGI, D. AL-SAAD, T. SAWAF and A. GEBRAN, 1990, Crustal shortening in the Palmyride fold belt, Syria, and implications for movement along the Dead Sea fault system, *Tectonics*, **9**, 1369-1386.
- CLARKE, P.J., *et al.*, 1998, Crustal strain in central Greece from repeated GPS measurements in the interval 1989-1997, *Geophys. J. Int.*, **135**, 195-214. R.C.
- COURTILLOT, V., R. ARMIJO and P. TAPPONIER, 1987, The Sinia triple junction revisited, *Tectonophysics*, **141**, 181-190.
- DAVIES, R.R., P.C. ENGLAND, B.E. PARSONS, H. BILLIRIS, D. PARADISSIS and G. VEIS, 1997, Geodetic strain in Greece in the interval 1892-1992, *J. Geophys. Res.*, **102**, 24,571-24,588.
- DEMETS, C., R.G. GORDON, D.F. ARGUS and S. STEIN, 1990, Current plate motions, *Geophys. J. Int.*, **101**: 425-478.
- DEMETS, C., R.G. GORDON, D.F. ARGUS and S. STEIN, 1994, Effects of recent revisions to the geomagnetic reversal time scale on estimates of current plate motions, *Geophys. Res. Lett.*, **21**, 2191-2194.
- DZIEWONSKI, A.M., T.-A. CHOU and J.H. WOODHOUSE, 1981, Determination of earthquake source parameters from waveform data for studies of global and regional seismicity, *J. Geophys. Res.*, **86**, 2825-2852.
- EL-FIKY, G.S., 1998, Temporal change of the crustal deformation and interplate coupling in the Tohoku district, northeast Japan, -a New Approach, Ph. D. thesis, Fac. of Scien., Tokyo Univ.
- EL-FIKY, G.S. and T. KATO, 1999, Continuous distribution of the horizontal strain in the Tohoku district, Japan, deduced from least squares prediction, *J. of Geodynamics*, **27**: 213-236.
- EL-FIKY, G.S., T. KATO and Y. FUJII, 1997, Distribution of the vertical crustal movement rates in the Tohoku district, Japan, predicted by least-squares collocation, *J. of Geodesy*, **71**: 432-442.
- GORSHKOV, G.P., 1984, Regionalnaya Seismotektonika Territorii Yuga SSSR: Alpiiskii Poyas. Nauka, Moscow (in Russian).
- JACKSON, J., 1992, Partitioning of strike-slip and convergent motion between Eurasia and Arabia in eastern Turkey, *J. Geophys. Res.*, **97**, 12, 471-12, 479.
- JACKSON, J. and D.P. MCKENZIE, 1988, The relationship between plate motions and seismic tremors, and the rates of active deformation in the Mediterranean and Middle East, *Geophys. J.R. Astron. Soc.*, **93**, 45-73.
- JACKSON, J., HAINES, J. and W. HOLT, 1992, The horizontal velocity field in the deforming Aegean Sea region determined from the moment tensors of earthquakes, *J. Geophys. Res.*, **97**, 17, 657-17,684.
- JACKSON, J., P. HUCHON and J. GAULIER, 1994, A comparison of SLR and seismicity in the Aegean region. *Geophys. Res. Lett.* **21**, 2849-2852.
- JESTIN, F., P. HUNCHON and J.M. GAULIER, 1994, The Somalia plate and the East African rift

- system: Present-day kinematics, *Geophys. J. Int.*, **116**, 637-654.
- JOFFE, S. and Z. GARFUNKEL, 1987, Plate Kinematics of the circum Red Sea-A re-evaluation, *Tectonophysics*, **141**, 5-22.
- KAHLE, H.-G., M.V. MULLER, A. GEIGER, G. DANUSER, S. MEULLER, G. VEIS, H. BILLIRIS and D. PARADIZZIS, 1995, The strain field in NW Greece and the Ionian islands: Results inferred from GPS measurements, *Tectonophysics*, **249**, 41-52.
- KAHLE, H.-G., M.V. MULLER and G. VEIS, 1996, Trajectories of crustal deformation of western Greece from GPS observations 1989-1994, *Geophys. Res. Lett.* **23**, 677-680.
- KATO, T., G.S. EL-FIKY, E.N. OWARE and S. MIYAZAKI, 1998, Crustal strain in the Japanese islands as deduced from GPS dense array, *Geophys. Res. Lett.*, **25**: 3445-3448.
- LE PICHON, X., N. CHAMOT-ROOKE, S. LALLEMANT, R. NOOMEM and G. VEIS, 1995, Geodetic determination of kinematics of central Greece with respect to Europe: Implications for Eastern Mediterranean tectonics, *J. Geophys. Res.*, **100**, 12,675-12.
- MCCCLUSKY, S. *et al.*, 2000, Global Positioning System constraints on plate kinematics and dynamics in the Eastern Mediterranean and Caucasus, *J. Geophys. Res.*, **105**, 5695-5719.
- McKENZIE, D.P., 1970, Plate tectonics of the Mediterranean region, *Nature*, **226**, 239-243.
- McKENZIE, D.P., 1972, Active tectonics of the Mediterranean region, *Geophys. J.R. Astron. Soc.*, **30**, 109-185.
- MORITZ, H., 1962, Interpolation and prediction of gravity and their accuracy. Report No. 24, Inst. Geod. Phot. Cart., The Ohio State Univ., Columbus, U.S.A.
- MULLER, S. and H.-G., KAHLE, 1993, Crust-mantle evolution, structures and dynamics of the Mediterranean-Alpine region, In Contributions of Space Geodesy to Geodynamics: Crustal Dynamics, Geodyn. Ser., 23, edited by D.E. SMITH and D.L. TURCOTTE, pp. 249-298. AGU, Washington, D.C.
- MULLER, B., M. L. ZOBACK, K. FUCHS, L. MASTIN, S. GREGERSEN, N. PAVONI, O. STEPHENSON and C. LJUNGGREN, 1992, Regional patterns of tectonic stress in Europe, *J. Geophys. Res.*, **97**, 11783-11803.
- NOOMEN, R., T. SPRINGER, B. AMBROSIUS, K. HERZBERGER, D. KUIJPER, G. METS, B. OVERGAUW and K. WAKKER, 1996, Crustal deformations in the Mediterranean area computed from SLR and GPS observations, *J. Geodyn.*, **21**, 73-96.
- ORAL, M., R. REILINGER and M. TOKSOZ, 1992, Deformation of the Anatolian block as deduced from GPS measurements, Eos Trans. Am. Geophys. Union, Fall AGU Meet. Suppl. 73, 120.
- PAPASTAMATIOU, D. and N. MOUYARIS, 1986, The earthquake of April 30, 1954, in Sophades (Central Greece), *Geophys. J.R. Astron. Soc.*, **87**, 885-895.
- PAPAZACHOS, C. and A. KIRATZI, 1992, Formulation for reliable estimation of active crustal deformation and its application to central Greece, *Geophys. J. Int.*, **111**, 424-432.
- PAPAZACHOS, C. and A. KIRATZI, 1996, A detailed study of the active crustal deformation in the Aegean and surrounding area, *Tectonophysics*, **253**, 129-153.
- PAPAZACHOS, C., A. KIRATZI and B.C. PAPAZACHOS, 1992, Rates of active crustal deformation in the Aegean and the surrounding area, *J. Geodynamics*, **16** (3), 147-179.
- PETER, Y., H.-G., KAHLE, M. COCARD, G. VEIS, S. FELEKIS and D. PARADISSIS, 1998, Establishment of a permanent GPS network across the Kephallonia fault zone, Ionian islands, Greece, *Tectonophysics*, **294**, 253-260.

Crustal Strains in the Eastern Mediterranean and Middle East as Derived from GPS Observations

- PLAG, H.-P., *et al.*, 1998, Scientific objectives of current and future WEGENER activities, *Tectonophysics*, **294**, 177–223.
- REBAL, S., H. PHILIP and A. TABOUDA, 1992, Modern tectonic stress field in the Mediterranean region: evidence for variation in stress directions at different scales, *Geophys. J. Int.* **110**, 106–140.
- REILINGER, R., *et al.*, 1997 a, Global Positioning System measurements of present-day crustal movements in the Arabia-Africa-Eurasia plate collision zone, *J. Geophys. Res.*, **102**, 9983–9999.
- REILINGER, R., *et al.*, 1997 b, Preliminary estimates of plate convergence in the Caucasus collision zone from global positioning system measurements, *Geophys. Res. Lett.*, **24**, 1815–1818.
- RIZNICHENKO, YU. V. and E.A. DZHIBLADZE, 1974, Determination of the maximum possible earthquakes on the basis of comprehension data on the Caucasus Region. *Izv., Earth Phys.*, **5**, 64–85.
- ROBBINS, J.W., P.J. DUNN, M.H. TORRENCE and D.E. SMITH, 1995, Deformation in the Eastern Mediterranean, In Proceedings of the First Turkish Int. Sym. on Deformations, **2**, pp. 738–745, Chamber of Surv. Eng. Ankara, Turkey.
- ROYDEN, L., 1993, The tectonic extension of slab pull at continental convergent boundaries, *Tectonic*, **12**, 303–325.
- SMITH, D.E., R. KOLENIEWICZ, J.W. ROBBINS, P.J. DUNN and M.H. TORRENCE, 1994, Horizontal crustal motion in central and Eastern Mediterranean inferred from satellite laser ranging measurements, *Geophys. Res. Lett.*, **21**, 1979–1982.
- SONDER, L. and P. ENGLAND, 1989, Effects of temperature dependent rheology on large-scale continental extension, *J. Geophys. Res.*, **94**, 7603–7619.
- STRAUB, C. and H.-G. KAHLE, 1994, Global Positioning System (GPS) estimates of crustal deformation in the Marmara Sea region, northwest Anatolia, *Earth Planet. Sci. Lett.*, **121**, 495–502.
- STRAUB, C. and H.-G. KAHLE, 1995, Active crustal deformation in the Marmara Sea region, NW Anatolia, inferred from GPS measurements, *Geophys. Res. Lett.*, **22**, 2533–2536.
- STRAUB, C., H.-G. KAHLE and C. SCHINDLER, 1997, GPS and geologic estimates of tectonic activity in the Marmara Sea region, NW Anatolia, *J. Geophys. Res.*, **102**, 27587–27601.
- TAYMAZ, T., H. EYIDOĞAN and J. JACKSON, 1991, Source parameters of large earthquakes in the East Anatolian Fault Zone (Turkey), *Geophys. J. Int.*, **106**, 537–550.
- WESTAWAY, R., 1994, Present-day kinematics of the Middle East and Eastern Mediterranean, *J. Geophys. Res.*, **99**, 12,071–12,090.
- ZOBACK, M. L., 1992, First-and second-order pattern of stress in the lithosphere: the world stress map project, *J. Geophys. Res.* **97**, 11703–11728.

(Received July 10, 2000)

(Accepted August 29, 2000)